

Synthesis of diamond hexagonal nanoplatelets by microwave plasma chemical vapor deposition

Chun-An Lu*, Li Chang

Department of Materials Science and Engineering, National Chiao Tung University, 1001 Ta Hsueh Rd. Hsinchu, 30010 Taiwan, Province of China

Available online 3 October 2004

Abstract

Variation of diamond deposition with temperature gradient was studied using standing-up substrates embedded within the plasma ball in microwave plasma chemical vapor deposition (MPCVD). The substrate is a polycrystalline diamond coated with a 30-nm thick iron film before deposition. Surface morphologies of the deposits and their crystalline characteristics were characterized by scanning electron microscopy, transmission electron microscopy (TEM), and selected area diffraction. On the upper area of the specimen near the center of the plasma ball where the temperature is the highest (>1100 °C), formation of diamond nanoplatelets in hexagonal shape with a thickness of 20–60 nm and side length of several hundreds of nanometers is found. In the middle region, diamond nanoplatelets with some iron nanoparticles are observed. Around the bottom region with low temperature near the edge of the plasma ball, nanodiamonds, Fe nanoparticles, and carbon nanotubes coexisted. The relative temperature distributions of diamond and carbon nanotube growth are briefly discussed.

© 2004 Elsevier B.V. All rights reserved.

Keywords: Platelets; Electron microscopy; Nanotubes; Morphology

1. Introduction

Diamond has excellent properties such as large band gap, high temperature resistance, high thermal conductivity, chemical inertness, and the highest hardness [1]. In recent years, researches investigate fabrication and applications of nanostructured materials because of their excellent physical properties [2–4]. Nanodiamond has been regarded as a new material with full of potentiality in electronic, optical, and mechanical fields due to its unique properties, like good field emission efficiency, low optical absorption coefficient, and good adhesion to substrates [5–7].

Nanodiamond films have already been synthesized by using chemical vapor deposition (CVD) method. The CVD nanodiamond film is an excellent material for field emission device such as flat panel displays because of its low or negative electron affinity with excellent mechanical and

chemical properties [7,8]. However, the nanodiamond films are usually defective with cauliflower-like shape [9].

In addition, nanocrystalline diamond films are usually obtained from the mixtures of hydrogen–methane or nitrogen–methane by chemical vapor deposition [10–12]. The substrate is usually put underneath a plasma ball, and the synthesized diamond is found having a three-dimensional nanostructure. In this paper, two-dimensional diamond nanoplatelets with (110) plane were successfully synthesized by CVD with the reaction gas composed of only hydrogen and methane. The formation of diamond nanoplatelets reveals an unexplored area of CVD diamond crystal growth before.

2. Experimental

2.1. Substrate preparation and placement

Before the synthesis process of diamond nanoplatelets, a 40- μ m thick polycrystalline diamond film was deposited on

* Corresponding author. Tel.: +886 3 5712121x55373; fax: +866 3 5724727.

E-mail address: chunanlu.mse88g@nctu.edu.tw (C.-A. Lu).

a precleaned 6-in. silicon (100) wafer by hot-filament chemical vapor deposition followed by deposition of a 30-nm thick Fe film by dc sputtering. The size of the substrate is $10.0 \times 10.0 \text{ mm}^2$. The diamond nanoplatelets were synthesized on the substrate in a 2.45-GHz ASTeX microwave plasma chemical vapor deposition (MPCVD) system. The substrate was vertically placed on a molybdenum holder, and a tantalum wire hang on the wall of the chamber was used as electrode (ground) in a position perpendicular to the substrate. The distance between the electrode and the substrate was about 5.0 mm. The plasma ball and the relative geometric position of the substrate with the electrode in the CVD chamber are schematically shown in Fig. 1.

2.2. Experimental parameters of deposition and analysis method

The deposition of diamond includes three steps: reduction, bias, and growth. Ferric oxide on the sample surface formed after exposure of the sputtered Fe film in air can be reduced by H_2 plasma in the first step. During the bias step, a high concentration (4%) of CH_4 was introduced to enhance the nucleation of diamond under a negative bias of -200 V with the process pressure of 20 Torr. After the nucleation, growth started with 0.667% CH_4 concentration in H_2 . The microwave power and growth time were 800 W and 30 min, respectively. During the reaction process, the top of the substrate was located near the plasma ball center. The radius of plasma ball was about 10.0 mm. It was observed that both the corners and the top of the substrate were brighter than the rest of the areas. Temperatures at different heights on the substrate surface were measured by an optical pyrometer. Surface morphology and crystal structure of the deposits were identified by a JOEL JSM-6500F field-emission scanning electron microscope (SEM) and a Philips Tecnai 20 transmission electron microscopy (TEM). For the TEM specimen preparation, the sample was immersed in an ethanol solution and accompanied with ultrasonic treatment to disperse diamond nanoplatelets. This

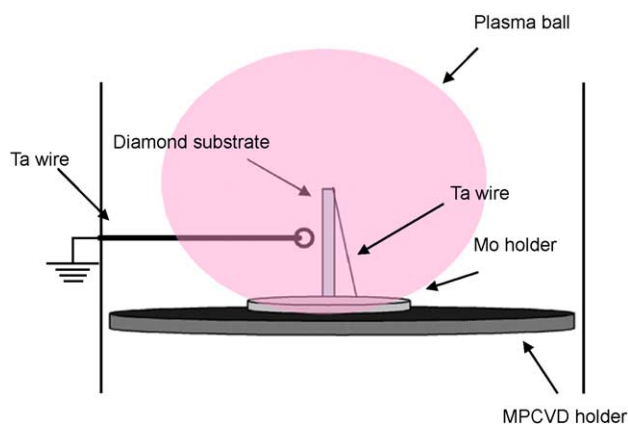


Fig. 1. Schematic diagram showing the arrangement of the substrate with respect to the plasma ball and the electrode of Ta wire.

diamond-dispersed solution was then dipped on a copper grid with a holey carbon film.

3. Results and discussion

Fig. 2(a) shows the surface morphology of the substrate before the MPCVD process. A polycrystalline and faceted surface is apparent. The average grain size is about 5–10 μm . After the MPCVD process, the substrate surface can be roughly divided into three different areas based on the morphology of deposited materials. The temperature distribution during the growth process at these three different positions of the substrate was over $1100 \text{ }^\circ\text{C}$ at the top area, about $1050\text{--}1080 \text{ }^\circ\text{C}$ at the middle area, and $1000 \text{ }^\circ\text{C}$ around the bottom area. A large quantity of interlaced nanoplatelets is found to be uniformly distributed over the top area of the specimen surface (Fig. 2(b)), where the temperature was the highest in these three areas. The density of the nanoplatelets is very high. Fig. 2(c) is a high-magnification image from which nanoplatelets in hexagonal-like morphology can be recognized with a thickness about 20–60 nm and a side length of 100–500 nm. It is noticed that most of the diamond nanoplatelets are oriented in a position perpendicular to the substrate surface. In the middle area of the substrate, the morphology in Fig. 2(d) shows that not only nanoplatelets are observed but also some nanoparticles exist here. From the higher magnification image of this area (Fig. 2(e)), the thickness and the side length of nanoplatelets are similar to the nanoplatelets in the upper area. The nanoparticles are identified to be iron particles, as shown in the following TEM result. Fig. 2(f) and (g) show the surface morphology on the bottom area. The diamond nanoplatelets are not found in this area. Instead, nanodiamond particles formed with an average size in the range of $\sim 10\text{--}100 \text{ nm}$. The iron nanoparticles and carbon nanotubes are also observed in this area. The result suggests that deposition at different areas in the plasma ball produces different carbon deposits with various morphologies. It is surprising to observe such significant variations just within the regions having temperature difference about $100 \text{ }^\circ\text{C}$, that is, from the top to the bottom regions on the substrate in the plasma ball. The distribution of temperature in a plasma ball known to have the highest temperature is near the center of the ball and gradually decrease from the center to the outside [13].

The diamond nanoplatelets were further analyzed by TEM. Fig. 3(a) is a bright-field (BF) TEM image obtained from the top area of the substrate. The characteristic morphology of crystalline platelet is seen in a hexagonal-like shape with facets. In addition to the nanoplatelet, some interlaced nanoplatelets were found near the upper left corner. The corresponding SAD pattern of the nanoplatelet in Fig. 3(b) exhibits cubic diamond single crystal diffraction pattern in $[110]$ zone axis. Additional spots are caused by the twins in the nanoplatelet. In the TEM sample, most of diamond nanoplatelets planes are close to $\langle 110 \rangle$ orientation

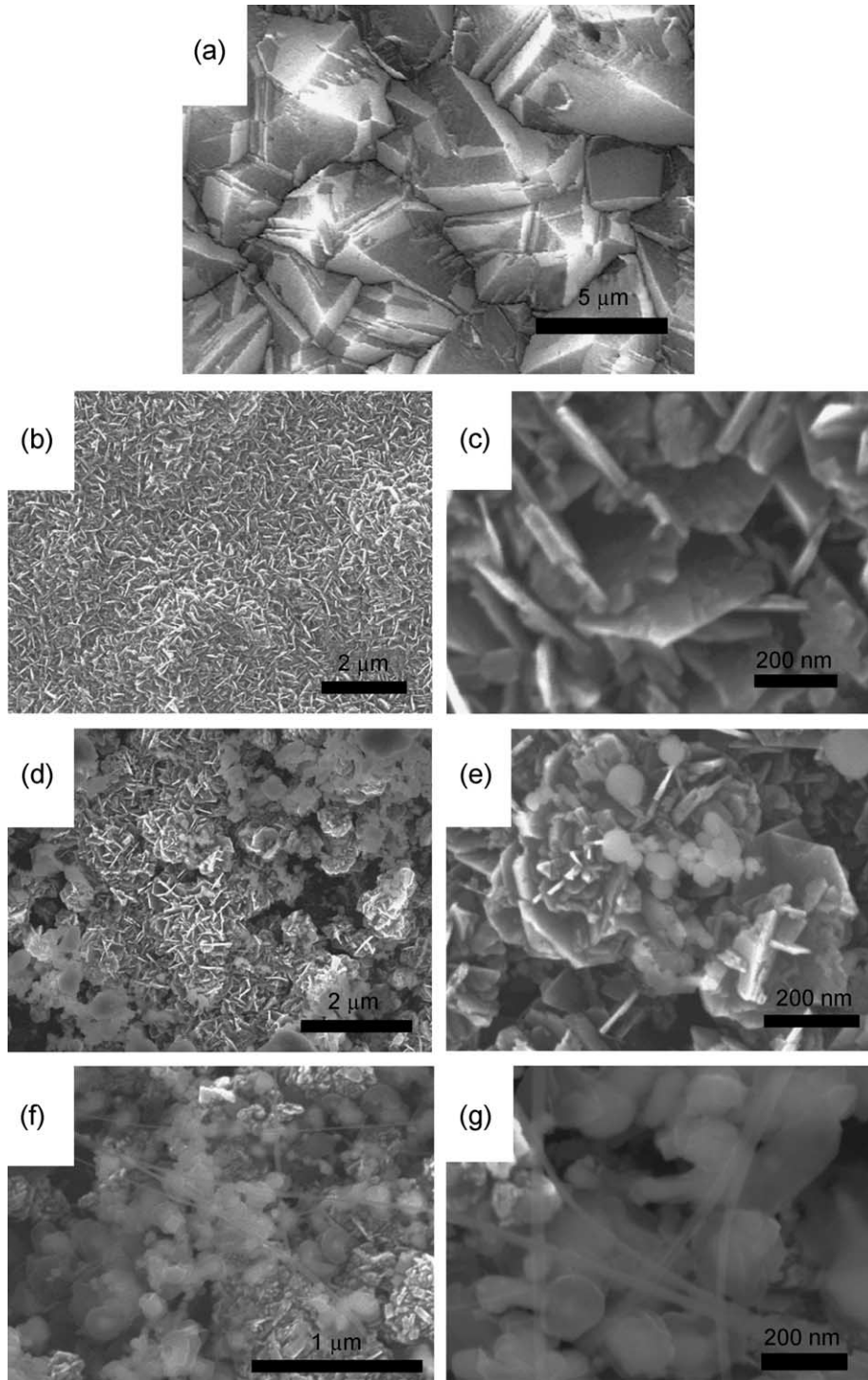


Fig. 2. SEM micrographs showing the surface morphology of (a) diamond substrate before MPCVD process, (b) the high-temperature area with high magnification in panel (c), (d) the middle-temperature area with high magnification in panel (e), and (f) and (g) the low-temperature area around the bottom of the sample.

as the nanoplatelet diamond plane was very easily tilted to $\langle 110 \rangle$ zone axis in an angle of $\sim 2\text{--}5$ degrees from zero degree after insertion of the sample in the TEM. According to the SAD, the facets can be ascribed to be $\{002\}$ and $\{111\}$. Fig. 3(c) shows the dark-field (DF) TEM image obtained from the 111 spot as pointed by white arrow shown

in Fig. 3(b). It can be seen that the platelet consists of some subunits with the same orientation.

Fig. 4(a) shows a BF TEM image acquired from the middle area of the substrate. The nearly hexagonal shape morphology of a crystalline platelet and a nanoparticle in 50–60-nm size near the nanoplatelet were found. The

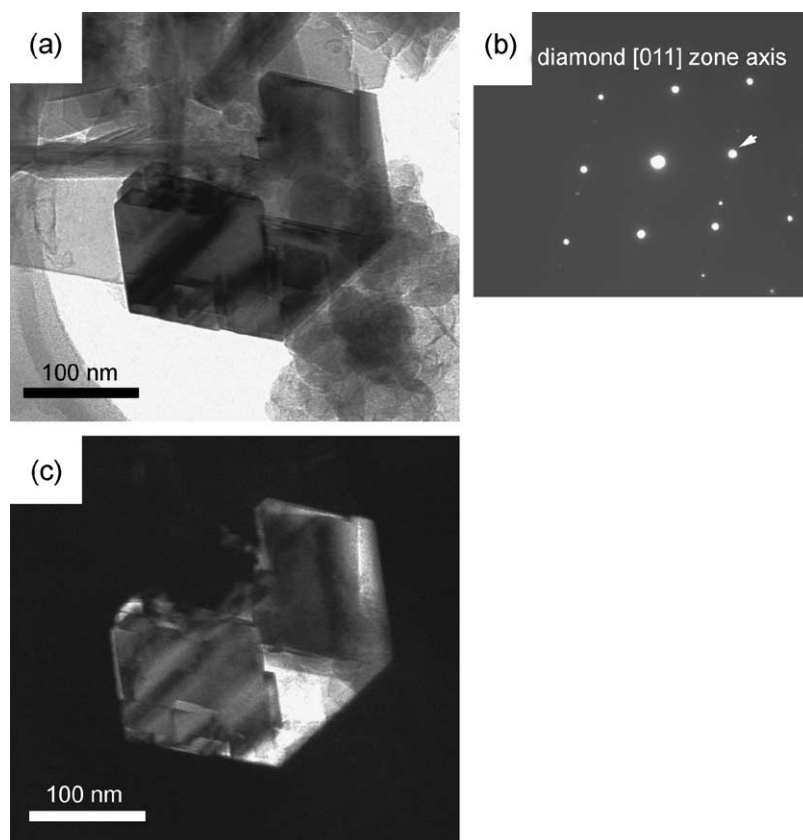


Fig. 3. (a) TEM image of a diamond platelet and (b) the electron diffraction pattern of the diamond in [011] zone axis. (c) Dark-field TEM image.

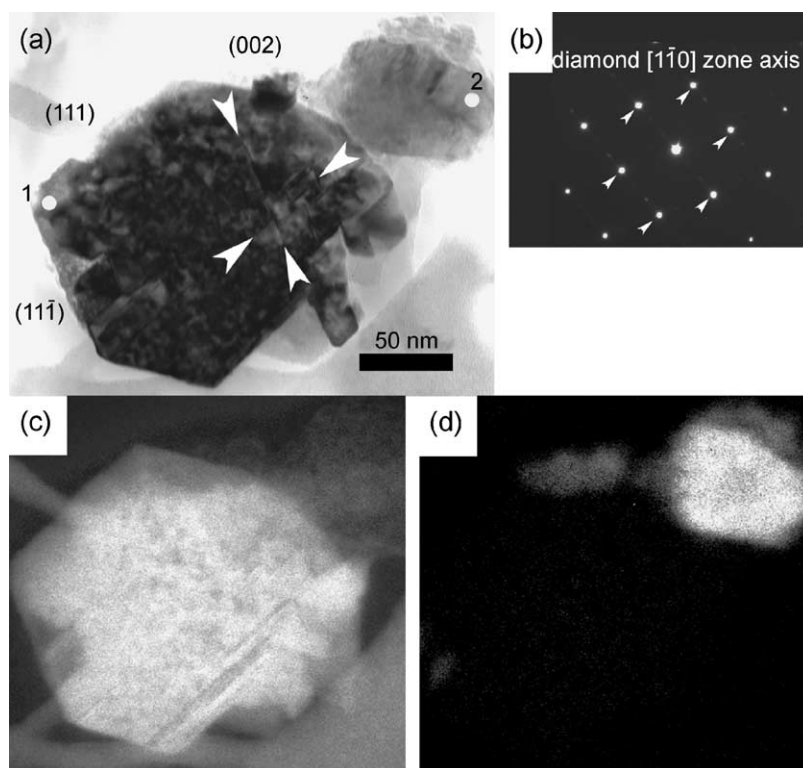


Fig. 4. (a) A bright-field TEM image of a diamond platelet and an iron nanoparticle and (b) showing the electron diffraction pattern of the diamond in [110] zone axis. (c) C map and (d) Fe map.

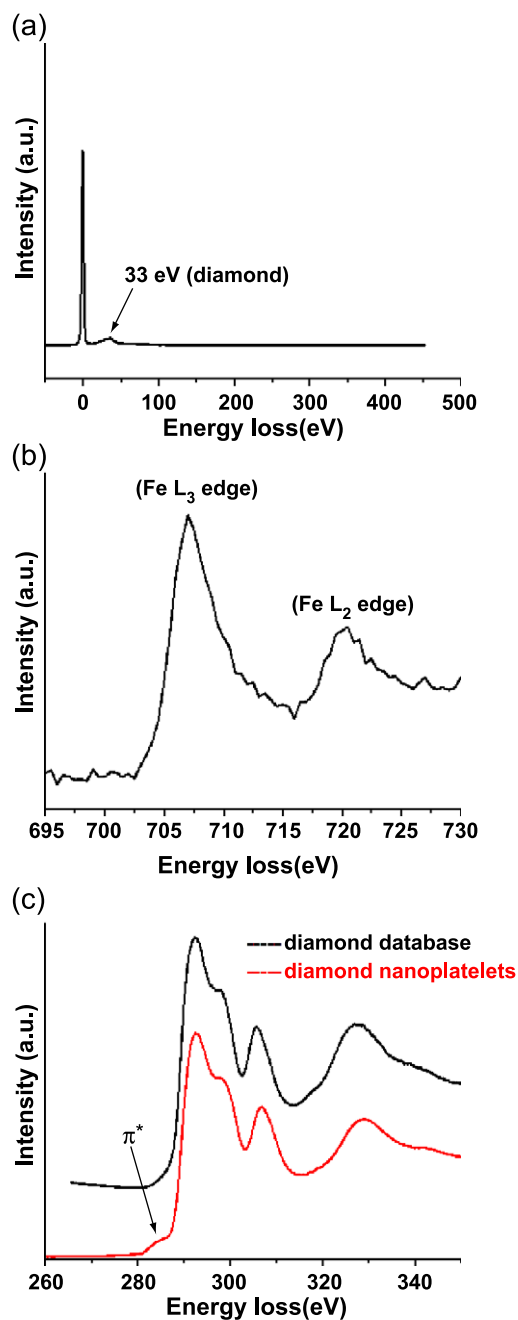


Fig. 5. EELS spectra. (a) The plasma region of a diamond nanoplatelet. (b) Fe $L_{2,3}$ edge from the Fe nanoparticle. (c) Carbon K edge of the diamond nanoplatelet in comparison with that of pure diamond.

corresponding SAD pattern of the nanoplatelet in Fig. 4(b) exhibits single crystalline diamond diffraction pattern in $[110]$ zone axis. Thus, contrast in the BF image Fig. 4(a) reveals that the diamond consists of multitwins parallel to the $\{111\}$ plane, as indicated by white arrowheads. The core loss signals of the carbon K edge (284 eV) and the iron L edge (708 eV) in an energy window of 10 eV were used for elemental mapping. Fig. 4(c) shows the carbon distribution in which the brightest area is corresponding to the diamond nanoplatelet region. Besides the diamond nanoplatelet area, other less bright areas from the holey carbon film on a

copper grid are also seen. A carbon-poor region on the upper right corner is also noticed to be corresponding to the nanoparticle. The Fe map in Fig. 4(d) shows that the intensity can be divided mainly in three levels in these crystals: the brightest is the Fe nanoparticle area, the gray region around the Fe nanoparticle is corresponding to iron carbide, and the darkest region is in the diamond nanoplatelet where no iron exists.

The chemical bonding state of diamond nanoplatelets can be determined by EELS technique. Fig. 5(a) shows the low-loss region of a spectrum acquired from spot 1 of Fig. 4(a). The plasmon peak at 33 eV is typical of diamond characteristics. The specimen thickness determined from log-ratio method from the low-loss region is about 43 nm,

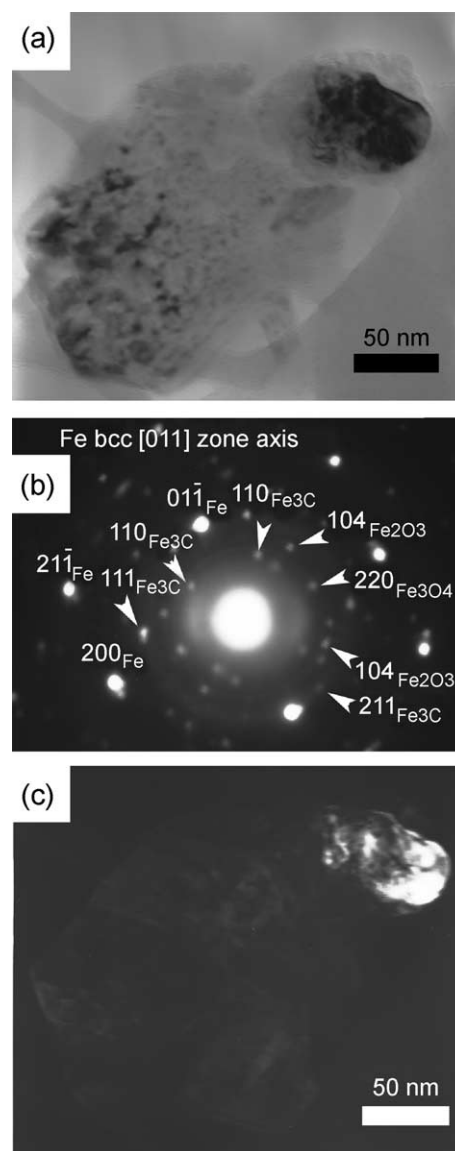


Fig. 6. (a) A bright-field TEM image of the same area as in Fig. 3 after tilting. (b) Selected area of electron diffraction pattern in $[110]$ zone axis of bcc Fe. The arrowed spots are reflections of Fe_3C iron carbide. (c) A dark-field TEM image of Fe nanoparticle.

consistent with SEM measurement. Fig. 5(b) shows the near edge structure of Fe L edge from the Fe nanoparticle in Fig. 4(a) (spot 2). In the spectrum, Fe L₃ and L₂ edges as white lines at 708 and 721 eV, respectively, are visible. Fig. 5(c) displays the comparison of the near edge structure of carbon K edge from a diamond nanoplatelet and a pure diamond particle. The peak at 285 eV corresponding to the π^* orbit of sp² carbon is probably due to contamination during electron beam irradiation.

To enhance the contrast of the iron nanoparticles, the TEM specimen was tilt away from diamond <110> zone axis. The BF image in Fig. 6(a) shows the iron nanoparticle in dark contrast. In the corresponding SAD pattern of Fig. 6(b), the six brightest diffraction spots are identified to be {111} and {200} reflections of body-centered cubic (bcc) iron in [011] zone axis. Other spots can be indexed as reflections from Fe₃C iron carbide and Fe₂O₃ iron oxide. The oxide is likely formed by oxidation of iron during the TEM specimen left in air. The iron carbide is probably the product of iron carburization in the deposition. Fig. 6(c) is a dark-field (DF) image taken from bcc Fe of 011 reflection, showing the Fe particle on the upper right corner. Another DF image taken from an Fe₃C reflection (not shown) reveals that the carbide particles are around the Fe nanoparticle.

According to the SEM results, the influence of temperature on diamond is apparent. It has been shown that the temperature at the center of a plasma ball can reach to ~2000–3000 °C in the cavity with hydrogen pressure of 100 mbar and microwave power of 1000 W [13]. In the present case, the diamond nanoplatelets formed at the place where the temperature was attained over 1100 °C during the MPCVD process. In contrast, diamond growth in conventional MPCVD process is in the temperature range from 700 to 900 °C, which often results in three-dimensional morphologies of polyhedrons.

Synthesis of carbon nanotubes has been extensively investigated since the first observation in 1991 [14]. It is now well known that the catalyst, reaction temperature, and reaction gas play important roles on formation of carbon nanotubes. Iron, cobalt, and nickel are known as the effective catalysts for the growth of carbon nanotubes [14–17]. The growth temperature range for carbon nanotubes is from 600 to 1000 °C [14–17]. When the growth temperature is over 1000 °C, hydrogen plasma will degrade the quality of carbon nanotubes with damage [15,17]. Moreover, it has been reported that the length and nucleation density of carbon nanotubes were reduced at 1000 °C, and highly defective carbon deposits are found on the substrate surface when the temperature was increased to 1100 °C [16]. In our case, the carbon nanotubes just formed on the low-temperature area (about 1000 °C). On the middle-temperature area (near the center of the substrate), the carbon nanotubes are not found, although iron catalyst was existed. At the highest-temperature area on the top of the substrate near the center of the plasma ball, diamond

crystals are the only deposit. Hence, it can be drawn that diamond can be synthesized from low temperature (900 °C) to high temperature (over 1200 °C), and nanotube can just be formed at lower temperature during MPCVD processing using methane and hydrogen gases. It is also worthwhile to point out that formation of carbon nanotubes in MPCVD system is generally in the condition of high concentration of methane at low temperature. But, in our case, we discovered that the carbon nanotubes could form in the deposition condition for diamond formation when iron exists at low methane concentration (CH₄ 0.667%) at temperature about 1000 °C.

4. Conclusion

Diamond deposition with temperature gradient was studied using standing-up substrates embedded within the plasma ball in MPCVD. On the upper area of the specimen near the center of the plasma ball where the temperature is highest (over 1100 °C), <110> oriented single crystalline diamond nanoplatelets were synthesized. The diamond nanoplatelets have a hexagon-like shape in with a thickness about 20 to 60 nm and length of several hundreds of nanometers. In the middle area of the sample with lower temperature (<1100 °C), the nanoplatelets and iron nanoparticles were coexistent. Around the bottom region at the lowest temperature (about 1000 °C), there exists diamond nanoparticles, iron nanoparticles, and carbon nanotubes as the deposits.

Acknowledgement

We thank the support from National Science Council, Taiwan, R.O.C. under contract of NSC92-2216-E009-020.

References

- [1] H. Liu, D.S. Dandy, *Diamond Chemical Vapor Deposition: Nucleation and Early Growth Stages*, Noyes Publications, New Jersey, 1995.
- [2] L.E. Brus, *J. Phys. Chem.* 98 (1994) 3575.
- [3] J. Rupp, R. Birringer, *Phys. Rev.*, B 36 (1987) 7888.
- [4] H. Gleiter, *Prog. Mater. Sci.* 33 (1989) 223.
- [5] X. Jiang, C.L. Jia, *Appl. Phys. Lett.* 80 (2002) 2269.
- [6] M.Q. Ding, W.B. Choi, A.F. Myers, A.K. Sharma, J. Narayan, J.J. Cuomo, J.J. Hren, *Surf. Coat. Technol.* 672 (1997) 94.
- [7] S.G. Wang, Q. Zhang, S.F. Yoon, J. Ahn, Q. Wang, D.J. Yang, Q. Zhou, Q.F. Huang, *Mater. Lett.* 56 (2002) 948.
- [8] D. He, L. Shao, W. Gong, E. Xie, K. Xu, G. Chen, *Diamond Relat. Mater.* 9 (2000) 1600.
- [9] D. Shechtman, A. Feldman, M.D. Vaudin, J.L. Hutchison, *Appl. Phys. Lett.* 62 (1993) 487.
- [10] C. Zuiker, A.R. Krauss, D.M. Gruen, X. Pan, J.C. Li, R. Csencsits, A. Erdemir, C. Bindal, G. Fenske, *Thin Solid Films* 270 (1995) 154.
- [11] K. Chakrabarti, R. Chakrabarti, K.K. Chattopadhyay, S. Chaudhuri, A.K. Pal, *Diamond Relat. Mater.* 7 (1998) 845.

- [12] D. Zhou, A.R. Krauss, L.C. Qin, T.G. McCauley, D.M. Gruen, T.D. Corrigan, R.P. Chang, H. Gnaser, *J. Appl. Phys.* 82 (1997) 4546.
- [13] H. Rau, B. Trafford, *J. Phys. D: Appl. Phys.* 23 (1990) 1637.
- [14] S. Iijima, *Nature (Lond.)* 354 (1991) 56.
- [15] C. Wei, K. Cho, D. Srivastava, *Mater. Res. Soc. Symp. Proc.* 677 (2001) AA6.5.
- [16] H. Cui, G. Eres, J.Y. Howe, A. Piretkzy, M. Varela, D.B. Geohegan, D.H. Lowndes, *Chem. Phys. Lett.* 374 (2003) 222.
- [17] Ch. Täschner, F. Pácal, A. Leonhardt, P. Spatenka, K. Bastsch, A. Graff, R. Kaltofen, *Surf. Coat. Technol.* 174–175 (2003) 81.